

Association Between Fluid Volume in Inner Nuclear Layer and Visual Acuity in Diabetic Macular Edema



KOTARO TSUBOI, QI SHENG YOU, YUKUN GUO, JIE WANG, CHRISTINA J. FLAXEL, STEVEN T. BAILEY, DAVID HUANG, YALI JIA, AND THOMAS S. HWANG

- **PURPOSE:** In diabetic macular edema (DME), the correlation between visual acuity (VA) and central subfield thickness (CST) is weak. We hypothesize that fluid volume (FV) in the inner nuclear layer (INL) may correlate more strongly with VA.

- **DESIGN:** Retrospective, cross-sectional study.

- **METHODS:** One eye each of diabetic patients with DME was included. We measured intraretinal fluid volume that was detected by automated fluid detection algorithm on 3- \times 3-mm optical coherence tomography angiogram volume scans. The detected fluid was subdivided into inner FV, bounded by the INL, and outer FV, the fluid between the outer border of INL to the ellipsoid zone.

- **RESULTS:** We enrolled 125 patients with DME (60 women; mean age, 61 years). The mean detected inner FV was 0.013 mm³ in 109 eyes (87%). The mean detected outer FV was 0.042 mm³ in 124 eyes (99%). Univariate analysis demonstrated that the VA significantly correlated with the inner FV ($P < .0001$), whole macular FV ($P = .010$), and CST ($P = .036$). Multivariate analysis demonstrated that the inner FV was the only significant factor ($\beta = -0.41$, $P = .004$). These correlations were consistent when the treatment-naïve group ($n = 33$) and the eyes without previous laser treatments ($n = 93$) were analyzed separately. The area under the receiver operating characteristic curve of inner FV for VA of 20/32 or worse was significantly higher than that for CST (0.66 vs 0.54, $P = .018$).

- **CONCLUSIONS:** The inner FV has a stronger association with VA than other OCT biomarkers in DME and may be more clinically useful. (Am J Ophthalmol 2022;237: 164–172. © 2021 Elsevier Inc. All rights reserved.)

Central subfield thickness (CST) is commonly used to measure the central macula in diabetic macular edema (DME). CST is the preferred optical coherence tomography (OCT) measurement because of its high reproducibility and correlation with other measures of the central macula.¹ In general, a thicker retina suggests a worse visual acuity (VA),^{2–6} but prior studies have reported that correlation coefficients between CST and VA are low to moderate.^{6,7} In fact, eyes with a thickened macula can have excellent VA, and eyes with a macula of normal thickness also have decreased vision.⁵ A potential reason is that CST can vary substantially among healthy individuals.^{8–13} Another possibility is that retinal atrophy may obscure increased fluid in the macula.¹⁴ In the management of DME, having a biomarker that correlates more closely with VA may help clinicians make more meaningful treatment decisions.

Recently, a deep learning-based algorithm has allowed an accurate segmentation and quantification of 3-dimensional fluid volume (FV) in the retina from dense optical coherence tomography (OCT) angiography (OCTA) volume scans. Our group has demonstrated that an automated central macular FV may be more sensitive and specific in detecting DME than CST, especially in eyes with retinal atrophy.¹⁵ However, the correlation coefficient between central macular FV and VA was low at -0.303 , which was similar to that between CST and VA of -0.339 . Histopathologic studies reported that cystic changes in DME occur primarily in the inner nuclear layer (INL) and the outer plexiform layer (OPL).^{16–19} INL consists of various cell bodies, and the loss of this layer, known as disorganized retinal inner layers (DRIL), has been closely associated with VA.^{20–22} We hypothesize that the changes that result in increased FV in the INL may similarly have a significant impact on VA.

In the current study, we quantified FV in the INL and FV in the OPL separately. In addition, we quantified the remnant tissue volume in the INL and the outer retina (between OPL and ellipsoid zone line). Taking advantage of deep learning-based segmentation and quantification of FV, we examine candidates for the most meaningful (in terms of visual acuity association) OCT biomarkers in eyes with DME.

AJO.com Supplemental Material available at [AJO.com](https://www.ajocom.com).
Accepted for publication December 9, 2021.

From the Casey Eye Institute (K.T., Q.S.Y., Y.G., J.W., C.J.F., S.T.B., D.H., Y.J., T.S.H.), Oregon Health and Science University, Portland, Oregon, USA; Kresge Eye Institute (Q.S.Y.), Detroit Medical Center, Wayne State University, Detroit, Michigan, USA; Department of Biomedical Engineering (J.W., Y.J.), Oregon Health & Science University, Portland, Oregon, USA

Inquiries to Thomas S. Hwang, Casey Eye Institute, Oregon Health & Science University, 515 SW Campus Dr, Portland, OR 97239, USA.; e-mail: hwangt@ohsu.edu

METHODS

The data reported in this retrospective cohort study comprise cross-sectional analyses from 2 prospective OCTA ongoing studies (National Institutes of Health, National Eye Institute R01 EY027833) performed at Casey Eye Institute, Oregon Health Science University. The details of the studies have been published recently.^{15,23-25} The study adhered to the tenets of the Declaration of Helsinki and complied with the Health Insurance Portability and Accountability Act of 1996. The Oregon Health Science University Institutional Review Board approved the study. All participants provided a written informed consent to participate in the OCTA studies.

We included diabetic eyes with any fluid detected by a deep-learning algorithm in the 3- × 3-mm OCTA scan, aged between 18 and 85 years. The study excluded pregnant or lactating women, those unable to consent or cooperate with OCT or OCTA scans, or those with presence of significant nondiabetic ocular diseases such as age-related macular degeneration. We also excluded eyes with a history of intraocular surgery except cataract surgery within 4 months before enrollment. Eyes with recent intravitreal injections were included. Only 1 eye of each participant was included in the study.

All participants underwent a medical history inquiry, comprehensive clinical examinations, and ocular imaging. The clinical examinations included Early Treatment of Diabetic Retinopathy Study (ETDRS) protocol visual acuity, intraocular pressure, slitlamp biomicroscopy, and indirect binocular ophthalmoscopy. Imaging procedures included standard 7-field ETDRS color fundus photography, 6- × 6-mm macular structural OCT raster scans (19 horizontal B-scans, automatic real-time tracking [ART] function activated and set at average of 9 frames; Spectralis) and 3- × 3-mm macular OCTA volumetric (304 × 304 A lines) scans (Avanti, Optovue). A retinal specialist (T.H.) determined the severity of diabetic retinopathy based on standard 7-field ETDRS color fundus photos using the ETDRS severity scale.²⁶

CST, defined as the mean thickness within a 1-mm circle centered on the fovea, was measured on Spectralis structural OCT raster scans using instrument-embedded Heyex 6.8.3 software (Heidelberg Engineering). The segmentations of the internal limiting membrane (ILM) and retinal pigment epithelium-Bruch membrane were manually checked for accuracy. A custom deep learning-based algorithm automatically quantified overall macular FV, including intraretinal and subretinal fluids, on 3- × 3-mm Optovue volumetric OCTA scans.^{27,28} Detected intraretinal fluids were further divided into inner fluid and outer fluid based on retinal layer segmentations (Figure 1) manually checked and corrected by our customized software—COOL-ART.^{29,30} When a retinal layer could not be par-

tially identified, for example, a large cyst obscured a layer, the segmentation was generated to be a smooth connection between each frame.

Inner FV was fluid between the upper and bottom border of INL, and outer FV was fluid between the bottom border of INL and the ellipsoid zone line. If a large cystoid space appeared to be a fusion of inner fluid and outer fluid due to an obscured boundary between INL and OPL, a large cystoid space was divided based on the segmentation. Subretinal FV was fluid between the ellipsoid zone line and retinal pigmental epithelium. We also measured remnant retinal tissue volume in the INL and in the outer retina. Retinal tissue volume in INL is inner FV subtracted from total volume between the upper and bottom border of INL, and retinal tissue volume in the outer retina is outer FV subtracted from total volume between the bottom border of INL and the ellipsoid zone line.

We also generated the 3- × 3-mm OCTA images acquired by the above OCTA system to measure the foveal avascular zone (FAZ) and vessel density (VD). The AngioVue OCTA software (version 2017.1.0.131) of the Avanti produced volumetric angiograms. A custom software COOL-ART^{29,30} further processed the volumes with a 3-dimensional projection resolved (PR)-OCTA algorithm.^{31,32} The FAZ was measured in the inner retinal slab, which included all structures between the ILM and OPL, using a custom MATLAB software (MathWorks).³³ The flow pixels in the en face angiogram of each plexus in a 3- × 3-mm scan area were counted and divided by the total number of pixels to yield the VD (units = percentage flow per area). We measured the VD in the superficial vascular complex (SVC), intermediate capillary plexus (ICP), and deep capillary plexus (DCP). SVC was defined as the inner 80% of the ganglion cell complex, which includes all structures between the ILM and inner plexiform layer/INL border, ICP was defined as the outer 20% of the ganglion cell complex to the inner 50% of the INL, DCP was defined as the outer 50% of the INL and the OPL.

We performed statistical analysis using JMP 13.2.0 software (SAS Institute, Inc) and GraphPad Prism (GraphPad Software). Normality assumption was assessed by normal probability plot and the Shapiro-Wilk test. We analyzed the relationships between VA and OCT parameters at the baseline visit using the Pearson correlation coefficient. Then, we performed a multivariate analysis with the least squares model including the variables with $P < .05$ in univariate analysis. The area under the receiver operating characteristic (AUROC) curve for VA of 20/32 or worse, which is one of the anti-vascular endothelial growth factor (VEGF) treatment criteria for DME,³⁴⁻³⁷ was calculated for CST and FV. The AUROC curves of CST and FV were compared using the method of DeLong et al.³⁸ $P < .05$ was considered as statistically significant.

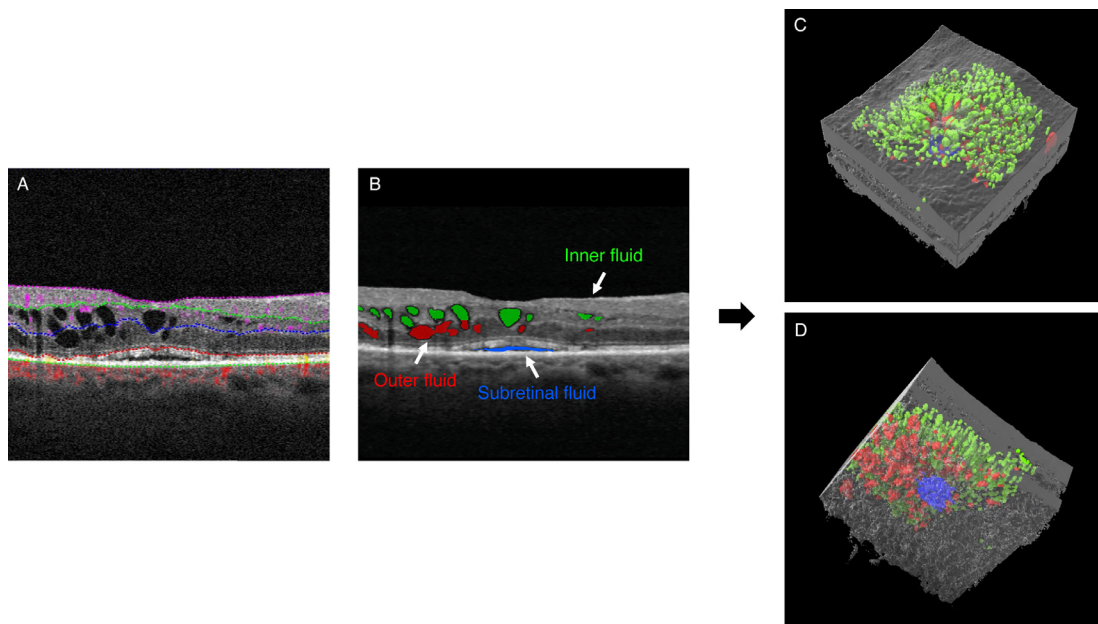


FIGURE 1. Fluid detection in each layer. **A.** Optical coherence tomography angiography B-scan image with segmentations. **B.** Inner fluid in green, outer fluid in red, and subretinal fluid in blue. **C and D.** Three-dimensional volume-rendered optical coherence tomography angiography with fluids. Inner fluid volume (FV) was 0.090 mm^3 , outer FV was 0.042 mm^3 , and subretinal FV was 0.0029 mm^3 .

RESULT

We enrolled 1 eye each of 125 patients (60 women [48%] and 65 men [52%]; mean age, 60.5 [SD, 11.8] years) with diabetes with any fluids detected by the algorithm in a 3×3 -mm OCTA scan area, including 1 without DR, 24 with mild nonproliferated DR (NPDR), 23 with moderate NPDR, 34 with severe NPDR, and 43 PDR (Table 1). The mean best-corrected VA was 76.6 (SD, 8.3) ETDRS letters (range, 49-93 ETDRS letters). The mean CST was 318 (SD, 75 μm ; 95% CI, 304-331 μm). Baseline clinical characteristics of patients are summarized in Table 1.

Of the 125 eyes, the inner fluid was observed in 109 eyes (87%) with a mean of 0.013 mm^3 (SD, 0.031 mm^3 ; 95% CI, 0.0072-0.019 mm^3), and 124 eyes (99%) had outer fluid with the mean outer FV of 0.042 mm^3 (SD, 0.088 mm^3 ; 5% CI, 0.027-0.058 mm^3). Subretinal fluid was observed in 29 eyes (23%), with a mean of 0.0020 mm^3 (SD, 0.0081 mm^3 ; 95% CI, -0.0011 to 0.0051 mm^3) (Table 1). Because of positive skewness (inner FV, 4.4; outer FV, 3.9; whole macular FV, 3.6), FV was used after base e-log transformation. The inner FV and outer FV correlated with CST ($R = 0.54$ and 0.57 , respectively). The outer FV was significantly greater than the inner FV ($P < .0001$ by paired t test).

The mean retinal tissue volume in INL was 0.35 mm^3 (SD, 0.066 mm^3 ; 95% CI, 0.34-0.36 mm^3), and the mean retinal tissue volume in outer retina, which is between OPL

and the ellipsoid zone line, was 1.09 mm^3 (SD, 0.20 mm^3 ; 95% CI, 1.05-1.12 mm^3). Because increased intraretinal FV may affect the surrounding remnant retinal tissue volume, we analyzed the relationship between FV and remnant retinal tissue volume in the same segmentation. There was a positive correlation between the inner FV, which exists in the INL, and retinal tissue volume in INL ($R = 0.42$; 95% CI, 0.25-0.56; $P < .0001$), as well as between the outer FV and retinal tissue volume in the outer retina ($R = 0.42$; 95% CI, 0.26-0.56; $P < .0001$).

Univariate analysis demonstrated that the VA correlated significantly with the inner FV ($R = -0.42$; 95% CI, -0.56 to -0.25) and the whole macular FV ($R = -0.23$; 95% CI, -0.39 to 0.056), but not with the outer FV. There was also significant correlation between CST and VA ($R = -0.19$; 95% CI, -0.35 to -0.013), which is much lower than the correlation between inner FV and VA. The retinal tissue volume in INL negatively correlated with VA ($R = -0.34$; 95% CI, -0.49 to -0.17), but the retinal tissue volume in outer retina did not (Figure 2). Between eyes with SRF ($n = 29$) and without SRF ($n = 96$), there was no difference in the mean VA (76.4 [SD, 1.5] vs 76.6 [SD, 0.8]; $P = .89$).

In the multivariate analysis, the inner FV (standard $\beta = -0.41$, $P = .004$), and the retinal tissue volume in INL (standard $\beta = -0.24$, $P = .024$) were the statistically significant factors. CST and the whole macular FV were not statistically significant (Table 2). When adjusted for the presence or absence of SRF, the inner FV (standard $\beta = -0.45$, $P < .0001$) remained a significant factor for the baseline VA.

TABLE 1. Baseline Demographic and Clinical Characteristics of the Study Participants

Parameter	Data Value (N = 125)
Age, y	60.5 (11.8) [28-80]
Sex, No.	
Men	65
Women	60
Most recent hemoglobin A _{1c} , %	7.8 (1.5) [5.7-14]
Blood pressure, mm Hg	
Systolic	132 (20) [89-195]
Diastolic	73 (14) [43-110]
History of hypertension, No. (%)	94 (79)
Axial length, mm Hg	23.6 (1.0) [21.2-26.3]
BCVA, ETDRS letter score	76.6 (8.3) [49-93]
DR stages, No. (%)	
Diabetes without DR (level <20)	1 (0.8)
Mild NPDR (level 20-35)	24 (19.2)
Moderate NPDR (level 43-47)	23 (18.4)
Severe NPDR (level 53)	34 (27.2)
PDR (level ≥61)	43 (34.4)
Previous treatment	(n = 92)
Anti-VEGF injection and/or steroid implant, No.	65
Focal macular photocoagulation, No.	32
Central subfield thickness, μm	318 (75) [180-670]
Foveal avascular zone, mm ²	0.33 (0.18) [0.031-1.02]
Vessel density in the	
Superficial vessel complex, %	36 (4.6) [25-46]
Intermediate capillary plexus, %	43 (3.7) [31-50]
Deep capillary plexus, %	43 (4.0) [32-51]
Fluid volume	
Inner (n = 109), mm ³	0.013 (0.031) [0-0.23]
Outer (n = 124), mm ³	0.042 (0.088) [0-0.61]
Whole macular (n = 125), mm ³	0.054 (0.10) [2.34 × 10 ⁻⁶ -0.73]
Subretinal (n = 29), mm ³	0.002 (0.008) [2.92 × 10 ⁻⁷ -0.043]
Retinal tissue volume in	
Inner nuclear layer, mm ³	0.34 (0.066) [0.23-0.55]
Outer retina, mm ³	1.09 (0.20) [0.66-2.28]

BCVA = best-corrected visual acuity; DR = diabetic retinopathy; ETDRS, Early Treatment Diabetic Retinopathy Study; PDR = proliferative diabetic retinopathy; SVC = superficial vessel complex; VEGF = vascular endothelial growth factor.

Note: Data are presented as the mean (SD) [range], unless otherwise indicated.

TABLE 2. Univariate and Multivariate Analysis for the Relationship Between Baseline Visual Acuity and Parameters

Parameters	Univariate Analysis		Multivariate Analysis		
	R (95% CI)	P Value	Estimation Value (95% CI)	Standard β	P Value
Fluid volume					
Inner	−0.42 (−0.56 to −0.25)	<.0001	−1.21 (−202 to −0.39)	−0.41	.0040
Outer	−0.17 (−0.34 to 0.0057)	.058			
Whole macular	−0.23 (−0.39 to −0.056)	.010	0.036 (−0.97 to 1.04)	0.0097	.94
Central subfield thickness	−0.19 (−0.35 to −0.013)	.036	0.014 (−0.011 to 0.040)	0.13	.27
Retinal tissue volume in					
Inner nuclear layer	−0.34 (−0.49 to −0.17)	.0001	−30.8 (−57.4 to −4.23)	−0.24	.024
Outer retina	−0.12 (−0.29 to 0.055)	.18	—	—	—

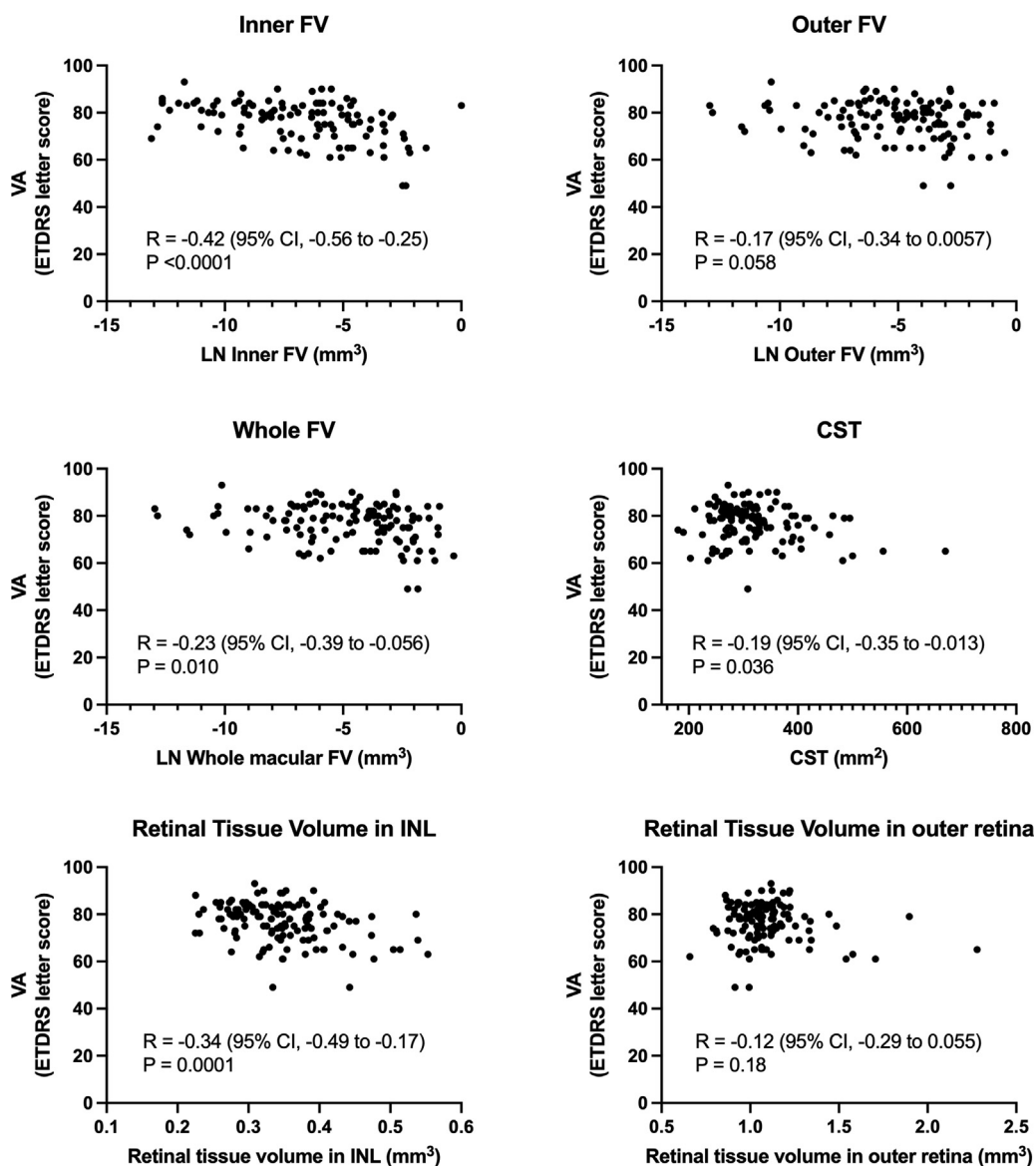


FIGURE 2. Scatter plots between baseline visual acuity (VA) and baseline parameters. Correlation coefficient and *P* values of the Pearson correlation coefficient are shown. CST = central subfield thickness; ETDRS = Early Treatment of Diabetic Retinopathy Study; FV = fluid volume; INL = inner nuclear layer; LN = Natural logarithm.

We also investigated the effects of macular ischemia using OCTA parameters, including FAZ and VD in the SVC, ICP, and DCP, on the relationship between inner FV and VA. There were no significant relationships between inner FV and OCTA parameters (all $P > .05$), except for a weak correlation between inner FV and VD in the DCP ($R = -0.19$, $P = .051$), suggesting the influence of cystic change on VD in the DCP. Univariate analysis showed a significant relationship between VA and VD in the SVC ($R = 0.37$, $P < .0001$), VD in the ICP ($R = 0.46$, $P < .0001$), and VD in the DCP ($R = 0.50$, $P < .0001$), but not with FAZ ($R = -0.11$, $P = .24$). When adjusted for these parameters, the relationship between inner FV and VA remained significant (Table 3).

When treatment-naïve eyes (33 eyes) or eyes without previous focal macular photocoagulation (PC) (93 eyes) were separately analyzed, the correlation between VA and inner FV remained the same (Table 4). This study included 42 eyes (34%) that received intravitreal injections (anti-VEGF drug in 41 eyes and steroid in 1 eye) within 4 months before the OCTA imaging. Subgroup analyses stratified by the presence or absence of DME treatment before the enrollment also demonstrated consistent results (Supplemental Table).

To investigate the clinical usefulness of the inner FV, we further analyze the diagnostic accuracy of the patients with VA of 20/32 or worse.³⁴⁻³⁷ The AUROC curve of inner FV for detecting eyes with VA of 20/32 or worse was 0.66,

TABLE 3. Relationship Between Inner Fluid Volume and Baseline Visual Acuity Adjusted for Optical Coherence Tomography Angiography Parameters

Model ^a	Parameters	Estimation Value (95% CI)	Standard β	P Value
1	Inner FV	−1.4 (−2.0 to −0.94)	−0.49	<.0001
	FAZ	−10 (−18 to −2.0)	−0.21	.015
2	Inner FV	−1.2 (−1.7 to −0.76)	−0.42	<.0001
	VD in the SVC	0.59 (0.29 to 0.88)	0.32	.0001
3	Inner FV	−1.1 (−1.6 to −0.69)	−0.39	<.0001
	VD in the ICP	0.97 (0.61 to 1.3)	0.42	<.0001
4	Inner FV	−0.99 (−1.5 to −0.53)	−0.34	<.0001
	VD in the DCP	0.94 (0.61 to 1.3)	0.45	<.0001

DCP = deep capillary plexus; FAZ = foveal avascular zone; FV = fluid volume; ICP = intermediate capillary plexus; SVC = superficial vascular complex; VA = visual acuity; VD = vessel density.

^aModel 1: Baseline VA = intercept + inner FV + FAZ; Model 2: Baseline VA = intercept + inner FV + VD in the SVC; Model 3: Baseline VA = intercept + inner FV + VD in the ICP; model 4: Baseline VA = intercept + inner FV + VD in the DCP.

TABLE 4. Correlations Between Visual Acuity and Parameters in Treatment-Naïve Eyes and Eyes Without Focal Macular Photocoagulation

Variable	Treatment-Naïve Eyes (n = 33)		Eyes Without Focal Macular PC (n = 93)	
	R (95% CI)	P Value	R (95% CI)	P Value
Fluid volume				
Inner	−0.45 (−0.71 to −0.097)	0.015	−0.39 (−0.56 to −0.19)	.0002
Outer	0.0048 (−0.34 to 0.35)	0.98	−0.23 (−0.42 to −0.027)	.027
Whole macular	−0.079 (−0.41 to 0.27)	0.66	−0.28 (−0.46 to −0.082)	.0063
Central subfield thickness	−0.0060 (−0.35 to 0.34)	0.97	−0.22 (−0.41 to 0.019)	.033
Retinal tissue volume in				
Inner nuclear layer	−0.35 (−0.62 to −0.011)	0.044	−0.36 (−0.52 to 0.16)	.0005
Outer retina	0.053 (−0.30 to 0.39)	0.77	−0.17 (−0.36 to 0.033)	.100

PC = photocoagulation.

whereas the AUROC curve of CST was 0.54 ($P = .018$). Eyes with VA of 20/32 or worse had significantly greater inner FV than eyes with VA of 20/30 or better ($0.022 \pm 0.042 \text{ mm}^3$ vs $0.0039 \pm 0.0099 \text{ mm}^3$, $P = .0025$ by Wilcoxon rank sum test). There was also a significant difference in the inner retinal tissue volume ($0.37 \pm 0.072 \text{ mm}^3$ vs $0.33 \pm 0.059 \text{ mm}^3$, $P = .0057$). However, there were no differences in CST, outer FV, or outer retinal tissue volume (all $P > .05$).

DISCUSSION

Retinal thickening is a key biomarker in the management of DME. A thicker retina usually means more severe disease, and many studies have reported a consistent correlation between VA and retinal thickness on OCT.²⁻⁶ Retinal thickness in DME is the sum of retinal tissue, cystic spaces, and subretinal fluid. FV may be a more specific indicator of ex-

udative changes in DME. A deep learning-based study examining retinal morphologic changes associated with VA in DME suggested that FV may be an important biomarker for VA.³⁹ Our previous study, however, demonstrated that the relationship between whole macular FV and VA was similar to the relationship between CST and VA. In the current study, we measured layer-specific FVs and found a stronger relationship between FV in the INL and VA compared with other OCT parameters.

The INL comprises numerous packed cells, including bipolar, amacrine, and horizontal cells. The presence of fluid in the INL may disrupt pathways that transmit visual information from the photoreceptor to the ganglion cells, as prior studies reported the association between the DRIL and VA.²⁰⁻²² The cystic spaces in the INL may also be caused by retrograde transsynaptic degeneration.⁴⁰ These may partially explain the close relationship between inner FV and VA.

The current results demonstrate the clinical value of the inner FV in the management of patients with DME. Center-involved patients with DME commonly present with good VA.⁴¹ Several clinical trials reported that the benefit of anti-VEGF injections for DME required VA loss of 20/32 or worse.³⁴⁻³⁷ The AUROC curve of inner FV for VA of 20/32 or worse was significantly higher than the AUROC curve of CST. Thus, the inner FV could be an alternative biomarker for monitoring patients with DME.

We also measured the remnant retinal tissue volume. Retinal tissue volume in INL also showed a negative correlation with VA. Inner and outer FV both positively correlated with the tissue volumes in the corresponding location. Although increased fluid may affect the measurement of retinal tissue volume due to a distortion and irregular segmentations, we speculate that an intracellular swelling and interstitial fluid that is below threshold for detection may cause the positive correlations between FV and tissue volume. Müller cells in pathologically altered retina due to diabetes displayed an osmotic swelling of their cell bodies.⁴² Müller cell swelling is also histologically observed in human diabetic eyes.⁴³ This intracellular swelling may lead to the increase of tissue volume. Another possibility is that the fluid undetectable by OCT exists in the remnant retinal tissue, as we observe a dye leakage on fluorescein angiography but no cystoid spaces on OCT.¹⁹ Therefore, we speculate that the increase in the tissue volume may suggest more swelling damage to the INL, and hence, has a negative impact on VA.

This study has several limitations. Our cohort included the eyes with intravitreal injections before OCTA imaging. Thus, it is necessary to consider the possibility that prior treatment may have affected the outcomes, despite subgroup analysis showing a consistent result. In addition, there was no difference in VA between eyes with and without SRF in this study, while a post hoc analysis of Diabetic

Retinopathy Clinical Research (DRCR) Protocol T found that the eyes with SRF had worse VA.⁴⁴ This difference may be because the Protocol T eyes had a worse mean VA of 64.8 letter scores⁴⁵ compared with this cohort, which had a mean VA of 76.6 letter scores. Thus, interpretation of the results should be made with caution.

The segmentation of inner FV and outer FV is challenging, even with deep learning–based algorithms. In this study, we used the fluid detection and segmentation algorithm based on high-definition OCTA scans with high sampling density. Although this algorithm is very accurate,^{28,46} diseased tissue can have poor structural boundaries, obscuring INL/OPL segmentation. Therefore, some segmentation of inner FV and outer FV may have been uncertain, especially in advanced disease, although we have manually corrected frame by frame. The positive correlation between FV and tissue volume suggests presence of the OCT undetectable intracellular swelling. The current algorithm can detect only cystic spaces, which must be a contiguous hyporeflective volume large enough to be detected. Nonetheless, both inner FV and tissue volume in the INL correlated with VA, suggesting swelling of INL, including both fluid and tissue volume, is important feature of worse VA in eyes with DME. The cross-sectional study design does not allow us to study changes in inner FV and VA over time, especially in response to treatment. Furthermore, it is not elucidated whether large fluid cysts induce tissue degeneration as reflected by changes like DRIL or whether degenerated retinal tissue allows larger cysts to form. Additional study is needed to better understand the relationship between tissue degeneration and fluid cysts in diabetic retinopathy.

In summary, inner FV may be a meaningful biomarker in the management of DME, which represents more specific pathologic changes in DME and has a stronger correlation with visual acuity compared with the commonly used CST. A longitudinal study is needed to validate the clinical utility of inner FV.

Funding/Support: This study was supported by the National Institutes of Health National Eye Institute (R01EY027833, R01EY024544, P30EY010572), William & Mary Greve Special Scholar Award, and unrestricted departmental funding from Research to Prevent Blindness (New York, NY). The funding source had no role in the design and conduct of the study; collection, management, analysis, and interpretation of the data; preparation, review, or approval of the manuscript; and decision to submit the manuscript for publication.

Financial Disclosures: Oregon Health & Science University (OHSU) and Yali Jia, Steven T. Bailey, and David Huang have a financial interest in Optovue Inc. OHSU and Yali Jia also have financial interest in Optos Inc. These potential conflicts of interest have been reviewed and are managed by OHSU. Kotaro Tsuboi has a financial interest unrelated to the current manuscript from Alcon Japan Ltd, Santen Co, Ltd, Novartis Pharma KK, and Bayer. The other authors indicate no financial support or conflicts of interest. All authors attest that they meet the current ICMJE criteria for authorship.

REFERENCES

1. Browning DJ, Glassman AR, Aiello LP, et al. Optical coherence tomography measurements and analysis methods in optical coherence tomography studies of diabetic macular edema. *Ophthalmology*. 2008;115(8):1366–1371 e1. doi:10.1016/j.ophtha.2007.12.004.
2. Hee MR, Puliafito CA, Wong C, et al. Quantitative assessment of macular edema with optical coherence tomography. *Arch Ophthalmol*. 1995;113(8):1019–1029. doi:10.1001/archophth.1995.01100080071031.
3. Hee MR, Puliafito CA, Duker JS, et al. Topography of diabetic macular edema with optical coherence tomography. *Ophthalmology*. 1998;105(2):360–370. doi:10.1016/s0161-6420(98)93601-6.
4. Otani T, Kishi S, Maruyama Y. Patterns of diabetic macular edema with optical coherence tomography. *Am J Ophthalmol*. 1999;127(6):688–693. doi:10.1016/s0002-9394(99)00033-1.

5. Browning DJ, Glassman AR. Diabetic Retinopathy Clinical Research Network. Relationship between optical coherence tomography-measured central retinal thickness and visual acuity in diabetic macular edema. *Ophthalmology*. 2007;114(3):525–536. doi:10.1016/j.ophtha.2006.06.052.
6. Bressler NM, Odia I, Maguire M, et al. Association between change in visual acuity and change in central subfield thickness during treatment of diabetic macular edema in participants randomized to aflibercept, bevacizumab, or ranibizumab: a post hoc analysis of the Protocol T Randomized Clinical Trial. *JAMA Ophthalmol*. 2019;137(9):977–985. doi:10.1001/jamaophthalmol.2019.1963.
7. Deák GG, Schmidt-Erfurth UM, Jampol LM. Correlation of central retinal thickness and visual acuity in diabetic macular edema. *JAMA Ophthalmol*. 2018;136(11):1215–1216. doi:10.1001/jamaophthalmol.2018.3848.
8. Dai W, Tham YC, Cheung N, et al. Macular thickness profile and diabetic retinopathy: the Singapore Epidemiology of Eye Diseases Study. *Br J Ophthalmol*. 2018;102(8):1072–1076. doi:10.1136/bjophthalmol-2017-310959.
9. Gupta P, Sidhartha E, Tham YC, et al. Determinants of macular thickness using spectral domain optical coherence tomography in healthy eyes: the Singapore Chinese Eye study. *Invest Ophthalmol Vis Sci*. 2013;54(13):7968–7976. doi:10.1167/iovs.13-12436.
10. Hashemi H, Khabazkhoob M, Yekta A, Emamian MH, Nabovati P, Fotouhi A. The distribution of macular thickness and its determinants in a healthy population. *Ophthalmic Epidemiol*. 2017;24(5):323–331. doi:10.1080/09286586.2017.1290808.
11. von Hanno T, Lade AC, Mathiesen EB, Peto T, Njølstad I, Bertelsen G. Macular thickness in healthy eyes of adults (N = 4508) and relation to sex, age and refraction: the Tromsø Eye Study (2007–2008). *Acta Ophthalmol*. 2017;95(3):262–269. doi:10.1111/aos.13337.
12. Tariq YM, Li H, Burlutsky G, Mitchell P. Ethnic differences in macular thickness. *Clin Exp Ophthalmol*. 2011;39(9):893–898. doi:10.1111/j.1442-9071.2011.02593.x.
13. Kelty PJ, Payne JF, Trivedi RH, Kelty J, Bowie EM, Burger BM. Macular thickness assessment in healthy eyes based on ethnicity using Stratus OCT optical coherence tomography. *Invest Ophthalmol Vis Sci*. 2008;49(6):2668–2672. doi:10.1167/iovs.07-1000.
14. Virgili G, Menchini F, Casazza G, et al. Optical coherence tomography (OCT) for detection of macular oedema in patients with diabetic retinopathy. *Cochrane Database Syst Rev*. 2015;1:CD008081. doi:10.1002/14651858.CD008081.pub3.
15. You QS, Tsuboi K, Guo Y, et al. Comparison of central macular fluid volume with central subfield thickness in patients with diabetic macular edema using optical coherence tomography angiography. *JAMA Ophthalmol*. 2021;139(7):734–741. doi:10.1001/jamaophthalmol.2021.1275.
16. Gass JD, Norton EW. Cystoid macular edema and papilledema following cataract extraction. A fluorescein fundoscopic and angiographic study. *Arch Ophthalmol*. 1966;76(5):646–661. doi:10.1001/archophth.1966.03850010648005.
17. Brownstein S, Orton R, Jackson B. Cystoid macular edema with equatorial choroidal melanoma. *Arch Ophthalmol*. 1978;96(11):2105–2107. doi:10.1001/archophth.1978.03910060485020.
18. Frangieh GT, Green WR, Engel HM. A histopathologic study of macular cysts and holes. *Retina*. 1981;1(4):311–336.
19. Otani T, Kishi S. Correlation between optical coherence tomography and fluorescein angiography findings in diabetic macular edema. *Ophthalmology*. 2007;114(1):104–107. doi:10.1016/j.ophtha.2006.06.044.
20. Sun JK, Lin MM, Lammer J, et al. Disorganization of the retinal inner layers as a predictor of visual acuity in eyes with center-involved diabetic macular edema. *JAMA Ophthalmol*. 2014;132(11):1309–1316. doi:10.1001/jamaophthalmol.2014.2350.
21. Sun JK, Radwan SH, Soliman AZ, et al. Neural retinal disorganization as a robust marker of visual acuity in current and resolved diabetic macular edema. *Diabetes*. 2015;64(7):2560–2570. doi:10.2337/db14-0782.
22. Das R, Spence G, Hogg RE, Stevenson M, Chakravarthy U. Disorganization of inner retina and outer retinal morphology in diabetic macular edema. *JAMA Ophthalmol*. 2018;136(2):202–208. doi:10.1001/jamaophthalmol.2017.6256.
23. Hwang TS, Jia Y, Gao SS, et al. Optical coherence tomography angiography features of diabetic retinopathy. *Retina*. 2015;35(11):2371–2376. doi:10.1097/IAE.0000000000000716.
24. Hwang TS, Gao SS, Liu L, et al. Automated quantification of capillary nonperfusion using optical coherence tomography angiography in diabetic retinopathy. *JAMA Ophthalmol*. 2016;134(4):367–373. doi:10.1001/jamaophthalmol.2015.5658.
25. You QS, Guo Y, Wang J, et al. Detection of clinically unsuspected retinal neovascularization with wide-field optical coherence tomography angiography. *Retina*. 2020;40(5):891–897. doi:10.1097/IAE.0000000000002487.
26. Early Treatment Diabetic Retinopathy Study Research Group. Grading diabetic retinopathy from stereoscopic color fundus photographs—an extension of the modified Airlie House classification. ETDRS report number 10. *Ophthalmology*. 1991;98(5 suppl):786–806.
27. Wang J, Zhang M, Pechauer AD, et al. Automated volumetric segmentation of retinal fluid on optical coherence tomography. *Biomed Opt Express*. 2016;7(4):1577–1589. doi:10.1364/BOE.7.001577.
28. Guo Y, Hormel TT, Xiong H, Wang J, Hwang TS, Jia Y. Automated segmentation of retinal fluid volumes from structural and angiographic optical coherence tomography using deep learning. *Transl Vis Sci Technol*. 2020;9(2):54. doi:10.1167/tvst.9.2.54.
29. Zhang M, Wang J, Pechauer AD, et al. Advanced image processing for optical coherence tomographic angiography of macular diseases. *Biomed Opt Express*. 2015;6(12):4661–4675. doi:10.1364/BOE.6.004661.
30. Guo Y, Camino A, Zhang M, et al. Automated segmentation of retinal layer boundaries and capillary plexuses in wide-field optical coherence tomographic angiography. *Biomed Opt Express*. 2018;9(9):4429–4442. doi:10.1364/BOE.9.004429.
31. Hwang TS, Zhang M, Bhavsar K, et al. Visualization of 3 distinct retinal plexuses by projection-resolved optical coherence tomography angiography in diabetic retinopathy. *JAMA Ophthalmol*. 2016;134(12):1411–1419. doi:10.1001/jamaophthalmol.2016.4272.
32. Zhang M, Hwang TS, Campbell JP, et al. Projection-resolved

- optical coherence tomographic angiography. *Biomed Opt Express*. 2016;7(3):816–828. doi:[10.1364/BOE.7.000816](https://doi.org/10.1364/BOE.7.000816).
33. Wang J, Hormel TT, You Q, et al. Robust non-perfusion area detection in three retinal plexuses using convolutional neural network in OCT angiography. *Biomed Opt Express*. 2019;11(1):330–345. doi:[10.1364/BOE.11.000330](https://doi.org/10.1364/BOE.11.000330).
 34. Brown DM, Nguyen QD, Marcus DM, et al. Long-term outcomes of ranibizumab therapy for diabetic macular edema: the 36-month results from two phase III trials: RISE and RIDE. *Ophthalmology*. 2013;120(10):2013–2022. doi:[10.1016/j.ophtha.2013.02.034](https://doi.org/10.1016/j.ophtha.2013.02.034).
 35. Do DV, Nguyen QD, Boyer D, et al. One-year outcomes of the da Vinci Study of VEGF trap-eye in eyes with diabetic macular edema. *Ophthalmology*. 2012;119(8):1658–1665. doi:[10.1016/j.ophtha.2012.02.010](https://doi.org/10.1016/j.ophtha.2012.02.010).
 36. Elman MJ, Aiello LP Diabetic Retinopathy Clinical Research Network. Randomized trial evaluating ranibizumab plus prompt or deferred laser or triamcinolone plus prompt laser for diabetic macular edema. *Ophthalmology*. 2010;117(6):1064–1077 e35. doi:[10.1016/j.ophtha.2010.02.031](https://doi.org/10.1016/j.ophtha.2010.02.031).
 37. Flaxel CJ, Adelman RA, Bailey ST, et al. Diabetic Retinopathy Preferred Practice Pattern®. *Ophthalmology*. 2020;127(1):P66–P145. doi:[10.1016/j.ophtha.2019.09.025](https://doi.org/10.1016/j.ophtha.2019.09.025).
 38. DeLong ER, DeLong DM, Clarke-Pearson DL. Comparing the areas under two or more correlated receiver operating characteristic curves: a nonparametric approach. *Biometrics*. 1988;44(3):837–845.
 39. Gerendas BS, Bogunovic H, Sadeghipour A, et al. Computational image analysis for prognosis determination in DME. *Vision Res*. 2017;139:204–210. doi:[10.1016/j.visres.2017.03.008](https://doi.org/10.1016/j.visres.2017.03.008).
 40. Lujan BJ, Horton JC. Microcysts in the inner nuclear layer from optic atrophy are caused by retrograde trans-synaptic degeneration combined with vitreous traction on the retinal surface. *Brain*. 2013;136(Pt 11):e260. doi:[10.1093/brain/awt154](https://doi.org/10.1093/brain/awt154).
 41. Early Treatment Diabetic Retinopathy Study Research Group Early Treatment Diabetic Retinopathy Study design and baseline patient characteristics. ETDRS report number 7. *Ophthalmology*. 1991;98(5 suppl):741–756. doi:[10.1016/s0161-6420\(13\)38009-9](https://doi.org/10.1016/s0161-6420(13)38009-9).
 42. Reichenbach A, Wurm A, Pannicke T, Iandiev I, Wiedemann P, Bringmann A. Müller cells as players in retinal degeneration and edema. *Graefes Arch Clin Exp Ophthalmol*. 2007;245(5):627–636. doi:[10.1007/s00417-006-0516-y](https://doi.org/10.1007/s00417-006-0516-y).
 43. Fine BS, Brucker AJ. Macular edema and cystoid macular edema. *Am J Ophthalmol*. 1981;92(4):466–481. doi:[10.1016/0002-9394\(81\)90638-3](https://doi.org/10.1016/0002-9394(81)90638-3).
 44. Roberts PK, Vogl WD, Gerendas BS, et al. Quantification of fluid resolution and visual acuity gain in patients with diabetic macular edema using deep learning: a post hoc analysis of a randomized clinical trial. *JAMA Ophthalmol*. 2020;138(9):945–953. doi:[10.1001/jamaophthalmol.2020.2457](https://doi.org/10.1001/jamaophthalmol.2020.2457).
 45. Wells JA, Glassman AR Diabetic Retinopathy Clinical Research Network. Aflibercept, bevacizumab, or ranibizumab for diabetic macular edema. *N Engl J Med*. 2015;372(13):1193–1203. doi:[10.1056/NEJMoa1414264](https://doi.org/10.1056/NEJMoa1414264).
 46. Guo Y, Hormel TT, Pi S, et al. An end-to-end network for segmenting the vasculature of three retinal capillary plexuses from OCT angiographic volumes. *Biomed Opt Express*. 2021;12:4889–4900. doi:[10.1364/BOE.431888](https://doi.org/10.1364/BOE.431888).